



## Structural and magnetic properties of electrodeposited Cobalt nanowire arrays

S. Sharma<sup>a</sup>, A. Barman<sup>a,\*</sup>, M. Sharma<sup>b</sup>, L.R. Shelford<sup>c</sup>, V.V. Kruglyak<sup>c</sup>, R.J. Hicken<sup>c</sup>

<sup>a</sup> Department of Physics, Indian Institute of Technology Delhi, Hauz Khas, New Delhi-110016, India

<sup>b</sup> Centre for Applied Research in Electronics, Indian Institute of Technology Delhi, Hauz Khas, New Delhi-110016, India

<sup>c</sup> School of Physics, University of Exeter, Stocker Road, Exeter EX4 4QL, United Kingdom

### ARTICLE INFO

#### Article history:

Received 3 June 2009

Accepted 20 June 2009 by A.H. MacDonald

Available online 26 June 2009

#### PACS:

79.60.Jv

74.25.Ha

75.60.Ej

#### Keywords:

A. Magnetic nanowires

B. Electrodeposition

D. Magnetisation reversal

E. Magneto-optical Kerr effect

### ABSTRACT

Ordered magnetic nanowires have tremendous potential in future magnetic storage and high frequency magnetic logic devices. Here, we present the fabrication of ordered arrays of Cobalt nanowires by electrodeposition through porous polycarbonate membranes. Vertically and horizontally aligned nanowires were produced in presence of an external bias field during post deposition etching of the polycarbonate membrane. Structural and compositional analyses have been carried out to establish the material and structural purity. The magneto-optical Kerr effect was employed to measure the magnetic hysteresis loops for the nanowires assembled in the substrate plane. A good magneto-optical signal to noise ratio is observed with clean ferromagnetic hysteresis loops. The loops measured with external magnetic field applied parallel and perpendicular to the axis of the nanowires show a clear difference in the shape and the coercive field, indicating the effect of shape anisotropy in these samples. Micromagnetic simulations were performed to understand the experimental results and to obtain insight to the magnetization reversal mechanism in magnetic nanowires.

© 2009 Elsevier Ltd. All rights reserved.

### 1. Introduction

Magnetic nanostructures will form the building blocks for future magnetic data storage such as patterned and perpendicular magnetic media [1]. Beyond that they have tremendous potential for applications in magnetic field sensors [2] and magnetic logic devices [3] in which magnetic domain movement or spin waves may be used as an information carrier. Two very important aspects of nanomagnets are the fabrication of ordered arrays in a cost effective manner and to probe their static and dynamic magnetic properties by highly sensitive non destructive techniques. A lot of effort has been directed towards fabricating nanomagnet arrays by slow and expensive but precise techniques such as optical and electron beam lithography [4]. Recent developments of chemical [5,6] and electrochemical [7,8] methods combined with self assembly processes have fueled interest into the fabrication of ordered magnetic nanostructures. On the other hand reports on characterization of their structural and magnetic properties have also been started [5–8]. However, a lot more progress is required in the fabrication of ordered arrays of high aspect ratio nanomagnets in wire and rod shapes with

desired magnetic properties before they could be introduced into applications.

The magneto-optical Kerr effect (MOKE) [9,10] is a very popular technique for probing the static [11] and time-resolved [12–14] magnetization processes of nanomagnets and also due to its use in magneto-optical data storage. Static and time-resolved MOKEs have made use of array measurements due to the enhancement of the total MOKE signal from a large number of elements in an array falling within the area of a diffraction limited laser spot ( $\sim 1 \mu\text{m}$ ). This gives rise to a collective response due to the ensemble effect, which is reflected in the magnetic switching field distribution (SFD) [15], and collective precessional modes in magnetization dynamics [16]. If precessional switching has to be introduced in the read–write processes of magnetic data storage, the above issues must be understood and controlled. Very few studies of magnetization dynamics in nanomagnet arrays have been reported so far [12–14,16]. An interesting prospect lies in the measurement of static and dynamic magnetization processes of electrodeposited dipolar coupled magnetic nanowire arrays by magneto-optical Kerr effect. However, this requires an enhancement of the magneto-optical signal to noise ratio from electrodeposited nanomagnet arrays. Here, we report the fabrication of ordered Cobalt nanowires by templated electrodeposition and assembling of the freestanding nanowires vertically or horizontally on the plane of the substrate. We also report the measurement of magnetic hysteresis loops from those nanowires by MOKE. Finally, we discuss the magnetization reversal process in Cobalt nanowires with the aid of micromagnetic simulations.

\* Corresponding address: Department of Materials Science, S. N. Bose National Centre For Basic Sciences, Block JD, Sector III, Salt lake, Kolkata 700 098, India Tel.: +91 33 23355706; fax: +91 33 23353477.

E-mail address: [abarman@bose.res.in](mailto:abarman@bose.res.in) (A. Barman).

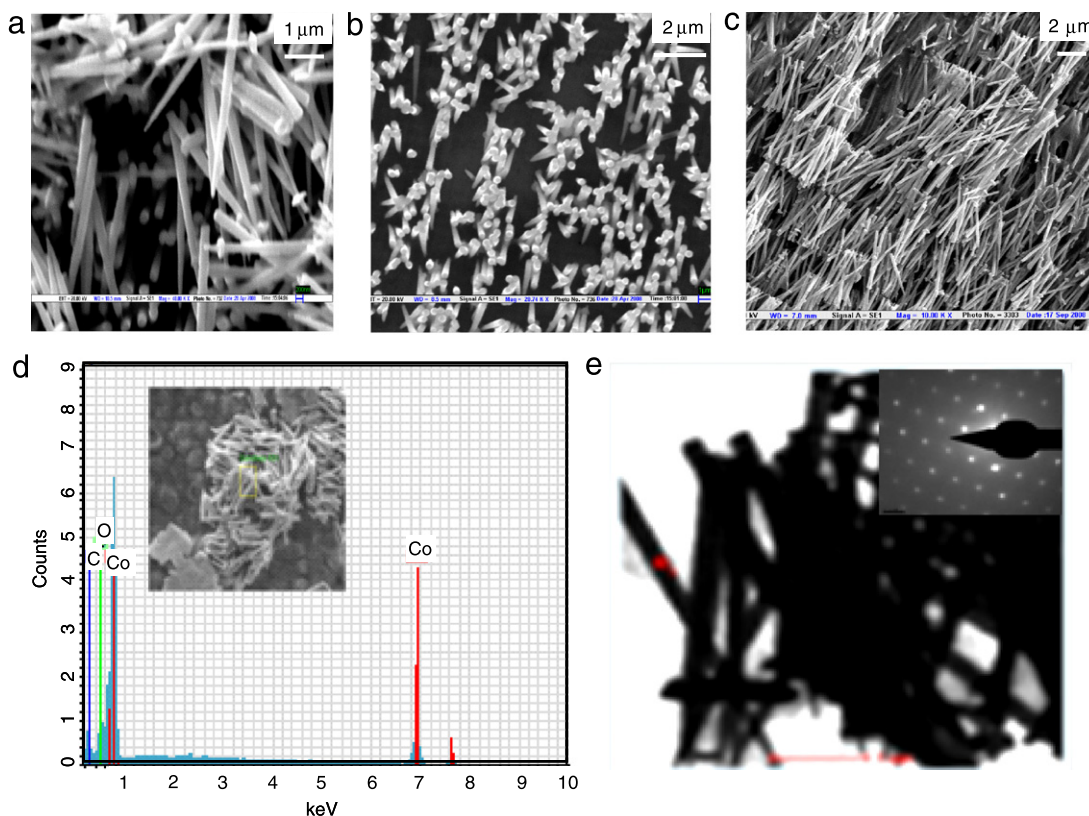


**Fig. 1.** Scanning electron micrographs of (a) freely lying nanowires (b) vertically aligned nanowires and (c) horizontally aligned nanowires of Cobalt on glass substrate after etching of the PCTE template. (d) Energy dispersive X-ray analysis of the composition of freely lying nanowires. (e) Selected Area Electron Diffraction (SAED) pattern from Transmission Electron Micrograph (TEM) of freely lying Cobalt nanowires.

## 2. Material and methods

Cobalt nanowire arrays were electrodeposited through commercially available polycarbonate track etched (PCTE) membranes with 100 nm diameter and thickness up to 6  $\mu\text{m}$ . The back side of PCTE was coated with a 100 nm thick Au layer which works as the working electrode for electrodeposition. Electrodeposition was performed in a bath of electrolyte and consists of 30 mM  $\text{CoSO}_4 \cdot 7\text{H}_2\text{O}$ , 120 mM  $\text{H}_3\text{BO}_3$  and 35 mM sodium lauryl sulphate. The deposition potential was first identified as  $-1.0$  V using cyclic voltametry and the deposition was carried out using chronoamperometry for different values of deposition time upto 500 s. Slower deposition rates and lower deposition potential were preferred for the better growth of the nanowires. Post deposition etching of the PCTE membrane was carried out by using dichloromethane and the freestanding nanowires were spread on a glass substrate. The etching was performed in the presence of a 4 kG magnetic field. A thin Au layer was deposited on a part of the nanowires after the template was etched and dried and scanning electron microscopy (SEM) was performed to investigate the morphology of the samples as shown in Fig. 1(a) to (c). The diameter of the nanowire is found to be around 100 nm and length up to 5  $\mu\text{m}$  for deposition time of 450 s. In absence of any magnetic field during etching no preferred orientation of the nanowires on the substrate is observed (Fig. 1(a)). When an out-of-plane magnetic field is applied sparse bunches of vertically aligned nanowires are observed (Fig. 1(b)) with irregular packing density mainly due to irregularity in the tracks in the PCTE membranes and insufficient out-of-plane magnetic field. However, well ordered horizontally aligned nanowires are formed (Fig. 1(c)) with a static in-plane magnetic field. A tendency towards formation of bundles is observed in both cases due to strong dipolar interaction between the wires.

The compositional analysis of the nanowires was performed by Energy Dispersive X-ray (EDX) attached with SEM and is shown in Fig. 1(d). The major elements present are Cobalt (84.37%), Carbon (7.49%) and Oxygen (8.14%). The Carbon content is most likely due to some residual organic solvent used at different stages of the sample preparation. The Oxygen content indicates that a slight oxidation may have occurred on the surface of the Cobalt nanowires, which is expected due to the absence of any protective layer on Cobalt. Fig. 1(e) shows the transmission electron micrograph (TEM) and selected area electron diffraction (SAED) pattern of the nanowires, which confirms a dominant hexagonal closed packed (hcp) crystalline structure of Cobalt. Previous reports have shown that a high melting point and higher binding energy of Cobalt favors the aggregation of atoms into small 3-D clusters which forms the Cobalt nanowires and can have c-axis orientation either parallel [17] or perpendicular [8,17] to the long axis of the nanowire depending on the pH of the electrolyte used during electrodeposition.

The hysteresis loops from the horizontally aligned nanowires were measured in the longitudinal MOKE geometry with the magnetic field applied within the plane of the sample. A linearly polarized laser with a wavelength of 632.8 nm was focused on a 200  $\mu\text{m}$  spot on the sample with an angle of incidence of about  $30^\circ$ . The reflected laser is scattered over a large solid angle due to sub-wavelength structures and irregularity of the surface of the electrodeposited sample. The reflected light was collected by a large aperture lens and collimated before being sent to an optical bridge detector consisting of a polarized beam splitter (PBS) and two photodiodes. The difference in the signal between the two photodiodes is proportional to the Kerr rotation [18]. The PBS is placed at  $45^\circ$  to the reflected light so that when a linearly polarized light (in the absence of Kerr rotation) passes through the PBS the intensity of light in two orthogonal components of polarization

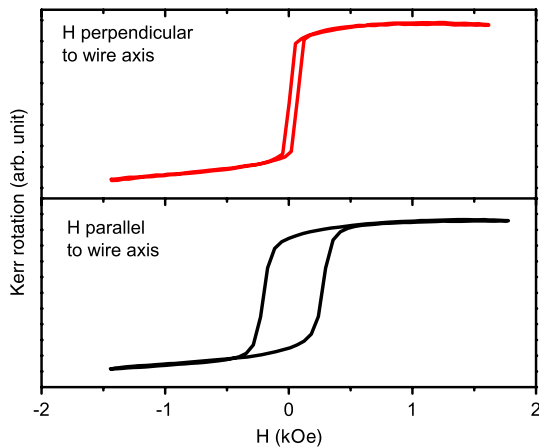


**Fig. 2.** Normalized magneto-optical Kerr rotation from horizontally aligned nanowires on glass substrate. The magnetic field was applied (a) perpendicular and (b) parallel to the wire axis.

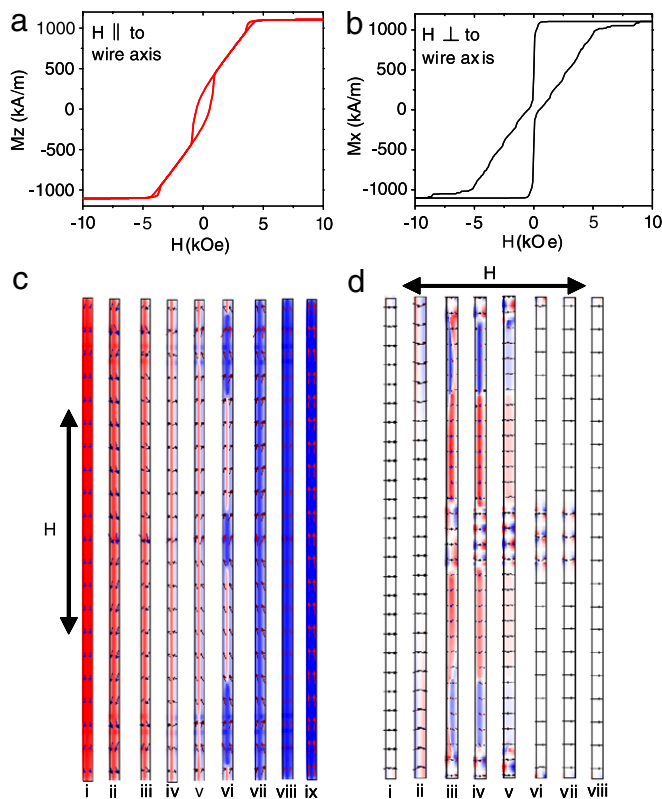


**Fig. 3.** Simulated hysteresis loops with  $H$  (a) parallel and (b) perpendicular to the axis of the nanowire. (c) Magnetization images of the nanowire for  $H$  parallel to wire axis at  $H =$  (i) 4 kOe, (ii) 1 kOe, (iii) 0, (iv)  $-0.56$  kOe, (v)  $-0.72$  kOe, (vi)  $-0.8$  kOe, (vii)  $-0.88$  kOe, (viii)  $-3.5$  kOe and (ix)  $-4.3$  kOe. (d) Magnetization images of the nanowire for  $H$  perpendicular to the wire axis at  $H =$  (i) 4.3 kOe, (ii) 5.6 kOe, (iii) 0, (iv)  $-4$  kOe, (v)  $-2$  kOe, (vi)  $-5.28$  kOe, (vii)  $-6.64$  kOe and (viii)  $-8.6$  kOe.

is identical, which gives rise to a ‘balance’ in the bridge. The Kerr rotation modifies the intensities in the two orthogonal components of polarization and gives rise to a finite electronic signal at the output of the optical bridge detector. The optical bridge detector eliminates the reflected light under the balanced condition and also amplifies the Kerr rotation signal when the difference in intensities in the two orthogonal components of polarization is measured. As a result it is a very sensitive technique and enables the measurements of clean hysteresis loops with very good signal to noise ratio. The hysteresis loops were measured with

a magnetic field applied parallel and perpendicular to the long axis of the nanowires.

### 3. Results and discussions

Fig. 2(a) and (b) show the hysteresis loops measured by longitudinal MOKE with magnetic field applied parallel and perpendicular to the direction of the long axis of the nanowires. There is a discernible change in the shape of the loops including the coercive field as the probe spot is moved over the sample area (not shown), which confirms the appreciable physical and magnetic inhomogeneity of the nanowire samples. However, despite that, loops with magnetic field applied parallel and perpendicular to the long axis of the nanowires are markedly different. The coercivity perpendicular to the wire axis is about 40 Oe, which is slightly higher than the bulk value (20 Oe) for Cobalt. It has been reported that for Cobalt nanowires with diameter  $>50$  nm the easy  $c$ -axis becomes perpendicular to the nanowire axis [8]. The increase in the coercive field for the nanowires perpendicular to the wire axis may be attributed to this. However, the coercivity increases to about 240 Oe parallel to the wire axis. The remanence does not vary significantly with the applied field orientation and is about 90% when the magnetic field is parallel to the wire axis and about 85% when the magnetic field is perpendicular to the wire axis. Although the EDX result shows more than 8% of Oxygen content probably due to slight oxidation of the surface of the nanowires, the loops do not exhibit any appreciable shift to show the presence of any exchange bias in the samples. The increase in coercive field for  $H$  parallel to the wire axis is most likely due to the shape anisotropy as a result of the high aspect ratio of the wires. For a uniformly magnetized cylindrical wire the demagnetizing field is  $H_d = (N_x - N_z) \times M_s$ , where  $N_x$  and  $N_z$  are the in-plane and out-of-plane components of the demagnetizing tensor and  $M_s$  is the saturation magnetization [19]. For a cylindrical Cobalt wire with aspect ratio  $\sim 50$  the above expression gives  $H_d \sim 8.7$  kOe. However, in reality a spatially periodic modulation of magnetization in Cobalt nanowires is observed as a result of competition between the magnetocrystalline polarization along the easy  $c$ -axis and the shape anisotropy energy along the wire axis [8,20]. The spatial modulation of magnetization reduces the demagnetizing energy and the resulting shape anisotropy and experimentally, a coercive field  $H_c$  of  $\sim 1$  kOe has been observed parallel to the wire axis for nanowire with an aspect ratio of  $>170$  [8]. Our observed value of  $H_c \sim 240$  Oe is smaller by a factor of 4. This is probably due to additional effects such as pinning of spins at the surface of the wire and the far from perfectly parallel alignment of the nanowires.

### 4. Micromagnetic simulations

We have further performed micromagnetic simulations on a single nanowire of 100 nm diameter and 5  $\mu\text{m}$  length by the public domain software Object Oriented Micro Magnetic Framework (OOMMF) [21] by discretizing the sample into rectangular parallelepiped cells of 5 nm  $\times$  5 nm  $\times$  10 nm size and with magnetic parameters as typical values for Cobalt. Fig. 3(a) and (b) show the simulated hysteresis loops with magnetic field ( $H$ ) applied parallel and perpendicular to the wire axis and are in sharp contrast with the experimental loops. When  $H$  is applied parallel to the wire axis the loop shows saturation field  $\sim 4.3$  kOe with small openings around the positive and negative saturation fields showing the signature of occurrence of magnetic vortex and a large opening around the zero field. The loop with  $H$  perpendicular to the wire axis is also vortex like but the centre of the loop is wide open showing the presence of additional domain structures. The magnetization images at different  $H$  values are shown in Fig. 3(c) and (d). When  $H$  is parallel to wire axis (Fig. 3(c)) and is less than

–4.3 kOe, the magnetization is parallel to the wire axis. At –4.3 kOe the magnetization switches to a vortex like structure with an extended core and the curling magnetization tilted towards the direction of the core forming a helical structure. The vortex core first switches in regions between the centre and edges at –800 Oe and then over the entire nanowire at –720 Oe. The curling magnetization slowly goes out of plane along the direction of the core with a further reduction of  $H$  and at  $H = 0$  the magnetization configuration is just opposite to what is seen for  $H = -880$  Oe. With a further increase in  $H$  the tilt angle of the curling magnetization increases and finally switches completely out of plane at +4.3 kOe. For  $H$  perpendicular to the wire axis the switching behavior is aided by the formation and annihilation of the vortex but takes a more complicated spatial distribution. Alternate regions along the length of the wire get divided into single vortex and double vortices of different core polarization and chirality and a flower like magnetization configuration. The reversal occurs in various regions of the nanowire at various field values starting near the ends of the nanowire at smaller  $H$  values ( $\sim 0.4$  kOe) and finally at the central region of the nanowire for higher field values ( $\sim 8.5$  kOe). The measured hysteresis loops are quite different from those obtained from the simulation for a single nanowire, which may be understood by the following effects. The strong inter-wire dipolar interaction may break down the vortex state and introduce more ordered magnetization and bulk like hysteresis loops. Moreover, defects and irregularities would modify the loops further. Finally slight overgrowth of the nanowire may have caused some regions of continuous films. The measurement of MOKE loops with a  $200 \mu\text{m}$  spot could sample a combination of the sheet film and the nanowires. Hence more detailed analysis and measurements are required to understand the magnetization reversal mechanism in arrays of dipolar coupled magnetic nanowires.

## 5. Conclusions

We have fabricated horizontally and vertically lying Co nanowires on a substrate by templated electrodeposition. The morphology, crystal structure and composition of the nanowires have been confirmed by SEM, TEM and EDX analyses. We have measured the magnetic hysteresis loops of the nanowires by magneto-optical Kerr effect measurements. A discernible difference is observed between the loops when  $H$  is applied parallel and perpendicular to the wire axis. However, the shape of the loops

and the coercive and saturation fields are significantly different from those obtained from micromagnetic simulations. We explain this disagreement by possible extrinsic effects such as strong inter-wire dipolar interaction, defects and irregularities of individual nanowires and those of the arrays.

## Acknowledgement

We gratefully acknowledge the financial support of UKIERI-DST standard research award (grant no. DST/INT/UKIERI/SA/P-2/2008) between IIT Delhi and the University of Exeter, UK.

## References

- [1] B.D. Terris, T. Thomson, *J. Phys. D: Appl. Phys.* 38 (2005) R199–R222.
- [2] E.A. Anderson, S. Isaacman, D.S. Peabody, E.Y. Wang, J.W. Canary, K. Kirshenbaum, *Nano Lett.* 6 (2006) 1160–1164.
- [3] D.A. Allwood, G. Xiong, C.C. Faulkner, D. Atkinson, D. Petit, R.P. Cowburn, *Science* 309 (2005) 1688–1692.
- [4] J.C. Lodder, *J. Magn. Magn. Mater.* 272 (2004) 1692–1697.
- [5] B. Martinez, X. Obradors, L. Balcells, A. Rouanet, C. Monty, *Phys. Rev. Lett.* 80 (1998) 181–184.
- [6] J. Park, J. Joo, S.G. Kwon, Y. Jang, T. Hyeon, *Angew. Chem. Int. Ed.* 46 (2007) 4630–4660.
- [7] A. Fert, L. Piroux, *J. Magn. Magn. Mater.* 200 (1999) 338–358.
- [8] Z. Liu, P.-C. Chang, C.-C. Chang, E. Galaktionov, G. Bergmann, J.G. Lu, *Adv. Func. Mater.* 18 (2008) 1573–1578.
- [9] J.M. Florczak, E.D. Dahlberg, *J. Appl. Phys.* 67 (1990) 7520–7525.
- [10] P. Kabos, A.B. Kos, T.J. Silva, *J. Appl. Phys.* 87 (2000) 5980–5982.
- [11] R.P. Cowburn, D.K. Koltsov, A.C. Adeyeye, M.E. Welland, *Appl. Phys. Lett.* 73 (1998) 3947–3949.
- [12] S. Jung, B. Watkins, L. DeLong, J.B. Ketterson, V. Chandrasekhar, *Phys. Rev. B* 66 (2002) 132401 (4 pages).
- [13] V.V. Kruglyak, A. Barman, R.J. Hicken, J.F. Childress, J.A. Katine, *Phys. Rev. B* 71 (2005) 220409 (4 pages).
- [14] K.S. Buchanan, X. Zhu, A. Meldrum, M.R. Freeman, *Nano Lett.* 5 (2005) 383–387.
- [15] O. Hellwig, A. Berger, T. Thompson, E. Dobisz, Z.Z. Bandic, H. Yang, D.S. Kercher, E.E. Fullerton, *Appl. Phys. Lett.* 90 (2007) 162516 (3 pages).
- [16] P.S. Keatley, V.V. Kruglyak, A. Neudert, E.A. Galaktionov, R.J. Hicken, J.R. Childress, J.A. Katine, *Phys. Rev. B* 78 (2008) 214412 (18 pages).
- [17] V.R. Caffarena, A.P. Guimaraes, W.S.D. Folly, E.M. Silva, J.L. Capitaneo, *Mater. Chem. Phys.* 107 (2008) 297–304.
- [18] P. Kasiraj, M. Shelby, J.S. Best, D.E. Horne, *IEEE Trans. Magn.* 22 (1986) 837–839.
- [19] A. Aharoni, *Introduction to the Theory of Ferromagnetism*, Clarendon, Oxford, 1996.
- [20] G. Bergmann, J.G. Lu, Y. Tao, R.S. Thompson, *Phys. Rev. B* 77 (2008) 054415 (5 pages).
- [21] M. Donahue, D.G. Porter, *OOMMF User's Guide*, Version 1.0, Interagency Report NISTIR 6376, National Institute of Standard and Technology, Gaithersburg, MD, 1999. URL: <http://math.nist.gov/oommf>.